Clinical Applications of Dual-Channel Transmit MRI: A Review

CME

Wyger M. Brink, MSc,[1] Vikas Gulani, MD, PhD,[2] and Andrew G. Webb, PhD[1]

This article reviews the principle of dual-channel transmit MRI and highlights current clinical applications which are performed primarily at 3 Tesla. The main benefits of dual-channel transmit compared with single-transmit systems are the increased image contrast homogeneity and the decreased scanning time due to the more accurate local specific absorption ratio estimation, meaning that less conservative safety limits are needed. The dual-transmit approach has been particularly beneficial in body imaging applications, and is also promising in terms of cardiac, spine, and fetal imaging. Future advances in transmit SENSE, the combination of dual-channel transmit with high permittivity pads, as well as the potential increase in the number of transmit channels are also discussed.

J. MAGN. RESON. IMAGING 2015;42:855–869.

Clinical MRI Scans, ideally, have uniform tissue contrast across the entire image. On 1.5 Tesla (T) and 3T systems the body coil is used for excitation, and is designed either as a birdcage[1] or transverse electromagnetic magnetic (TEM)[2] geometry, both of which provide a homogeneous radiofrequency (RF) transmit field (B_1) in an empty coil. However, the presence of the patient in the RF coil disturbs the uniformity of the RF transmit field, and results in areas within the body in which the transmit field is significantly weaker than in other regions. This perturbation increases as a function of the main magnetic field (B_0), the dimensions of the body part being imaged, and the relative permittivity (sometimes referred to as the dielectric constant) and conductivity of the tissue. A spatially varying transmit field produces corresponding variations in the flip angle within the body, and subsequent distortions in image contrast weighting. In extreme cases signal voids can occur in the image. Examples of image artifacts in breast, abdominal and cardiac scans at 3T are shown in Figure 1. Although some degree of intensity correction is possible using a direct measurement of the transmit field, these types of postprocessing schemes cannot recover any of the reduced tissue contrast due to spatially varying tip angles. Because these effects are more severe the higher the magnetic field, many clinical protocols which could potentially benefit from the intrinsically higher signal-to-noise ratio (SNR) at 3T continue to be run on 1.5T systems. Several review articles have addressed the considerations in determining which clinical applications are appropriate for which field strength.[3–6]

The major factor causing B_1-inhomogeneity is the high relative permittivity of the body. The wavelength of the RF waves in tissue is inversely proportional to the square root of the relative permittivity of the tissue. Figure 2 shows the relative permittivity of muscle, as well as the corresponding wavelength, as a function of field strength. In muscle, at 1.5T the wavelength is $\sim$52 cm, whereas at 3T it is $\sim$26 cm. This means that at 3T the dimensions of the body are a substantial fraction of the RF wavelength in tissue, and so the RF energy propagating through the body from different directions by means of the body coil produces areas of constructive and destructive interference, as shown schematically in Figure 3. The second factor which can cause B_1-inhomogeneity is tissue conductivity: increased conductivity corresponds to reduced RF penetration through tissue. As shown in Figure 2, this effect is not too severe with penetration depths of many tens of centimeters for healthy tissue at 1.5 and 3T. However, because conductivity increases with frequency (and, therefore, magnetic field strength) the effects become much more pronounced at 7T and above. A full mathematical description of the effects of permittivity and conductivity on the RF behavior in elliptical objects can be found, for example, in the publication by Sled and Pike.[7]

The relationship between body type and the degree of image artifacts involves several components. Obese patients typically show greater image inhomogeneity due to their larger body size. Pathological conditions such as ascites, in which large volumes of water accumulate, are particularly problematic due to the high relative permittivity. If fluid accumulations within the body also have high salt content, then image uniformity is further degraded due to the reduced penetration depth. However, as reported by many authors, image artifacts can also be substantial in very thin patients. This is because the cross-section of the body in these cases is highly elliptical, i.e., very asymmetric with respect to the circular body coil. There is very little that can be done to overcome these artifacts using a single transmit channel 3T
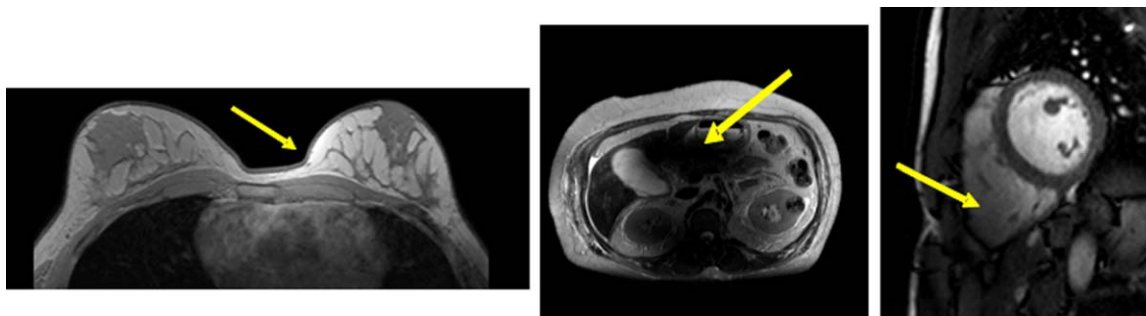
FIGURE 1: Examples of image artifacts at 3 Tesla. Left: Breast images showing unequal left/right signal intensity. Center: Anterior/posterior signal voids in abdominal imaging. Right: Shading artifacts in cardiac scans.
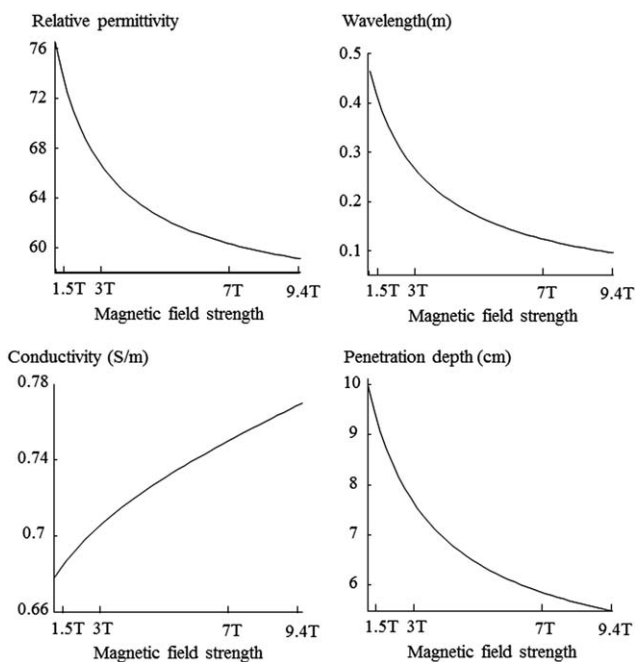
FIGURE 2: Plots of relative permittivity, wavelength, conductivity, and penetration depth for muscle tissue at different magnetic field strengths.

FIGURE 4: a: Single-channel transmit body coil operating in quadrature mode. There is a fixed phase angle of 90° between the two ports, and the amplitudes of the signal fed into each of the two ports are the same. b: Dual-channel transmit body coil. Using two separate transmitters, the amplitudes and phases of the two channels can be set independently, giving additional degrees of freedom.

scanner (Fig. 4a). Dielectric pillows containing water-based gels have been proposed,[8] and indeed image quality generally increases, but these pillows are large and heavy, placement is critical and patient comfort is compromised. New approaches using much thinner pads with very high permittivity materials[9] are discussed in the final section of this article.

The clinical importance of this situation has resulted in the recent introduction of commercial dual-channel transmit systems at 3T, in which the body coil is effectively split into two channels, each of which can be driven with an independently controlled magnitude and phase, as shown in

Figure 4b. The additional degrees-of-freedom (relative amplitudes and relative phases of the two channels) compared with a single degree-of-freedom (amplitude) for a conventional single transmit system can produce significant increases in RF transmit homogeneity, as has long been known theoretically. This approach of having extra degrees of freedom has been adapted from similar approaches in the area of electromagnetic hyperthermia,[10] and is considered in more detail in the following sections.

Single-Channel Transmit Versus Dual-Channel Transmit Approaches

In the conventional single-channel approach, Figure 4a, the body coil is driven in quadrature with equal magnitudes
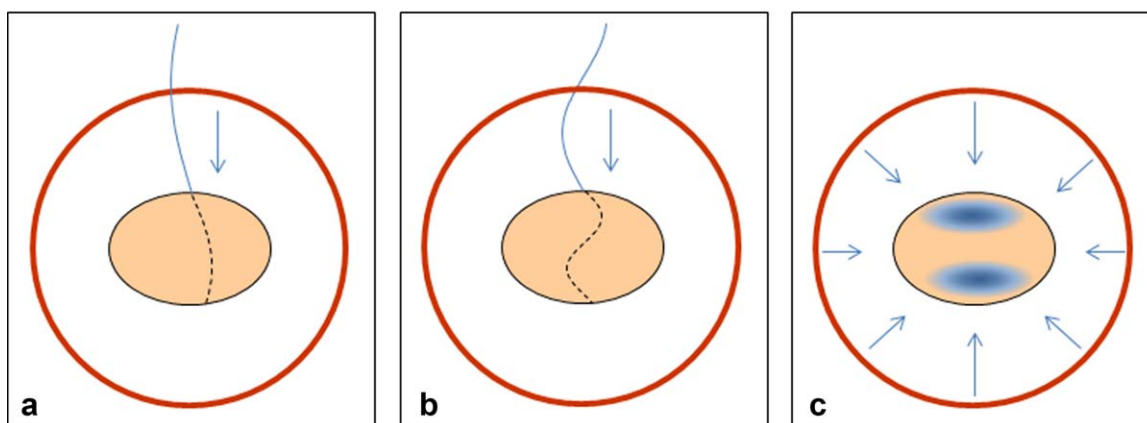
FIGURE 3: A schematic showing interference effects of the RF field in the body, represented as an ellipse, within the circular body coil (red circle). a: At 1.5T, the wavelength in air is ~235 cm, and in tissue ~52 cm. The tissue wavelength is larger than the body dimensions and, therefore, relatively little wave interference occurs. b: At 3T, the wavelength in air is ~117 cm, and ~26 cm in tissue. A much greater degree of wave interference is, therefore, seen than at 1.5 Tesla. c: This increased wave interference manifests itself as areas of low transmit efficiency (shaded regions).
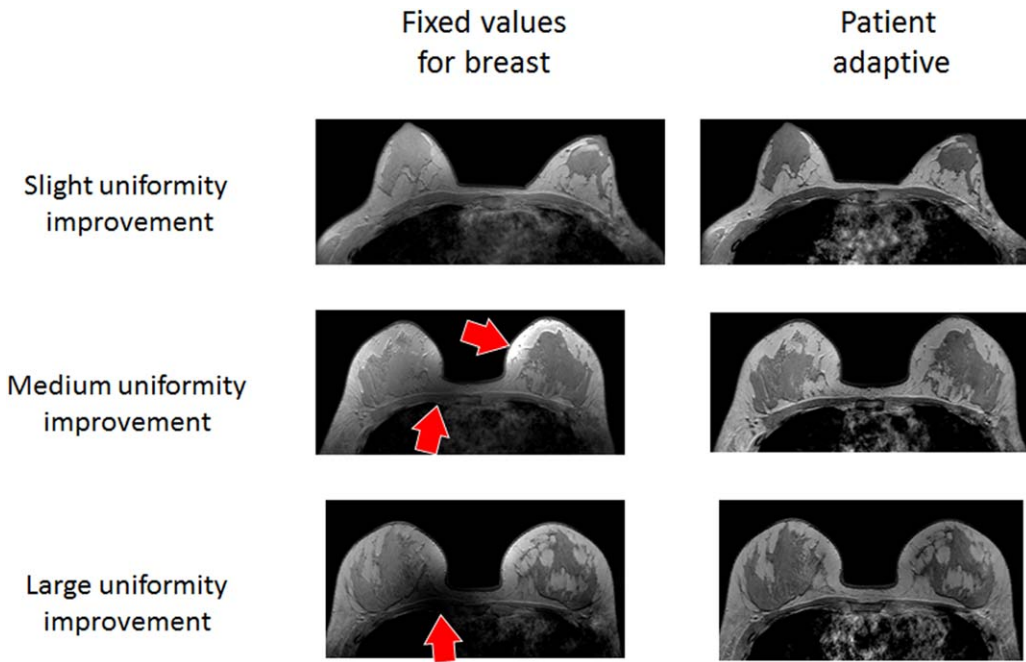
FIGURE 5: An illustration of the advantages of using patient-specific B$_1$-shimming for breast imaging compared with a generically optimized fixed amplitude/phase relationship. In the upper panel the fixed values give good image quality with no signal drop-outs or differential intensities in the left and right breasts: there is little difference between fixed and patient-specific values. However, in the lowest panel there are clear image artifacts produced by the fixed-value approach in a different subject with larger breast size. In contrast, by using patient-specific values of the amplitude and phase, good image quality can be obtained in all cases.

and a fixed 90° phase shift of the two signals fed into the two orthogonal ports of the coil. Although this mode is effective in terms of providing a homogeneous transmit field at low (≤1.5T) magnetic field strengths, this geometry is not optimal at 3T for a subject geometry which is essentially elliptical, and results in nonuniformities in the transmitted RF field. The dual-channel transmit approach forms a logical improvement to the single-channel system in that it uses two completely independent transmit chains for driving the two ports of the coil. Different amplitudes and phases of the RF pulses, as well as their waveforms, can be applied through these two independent channels. Initially it was thought that a limited number of fixed preset amplitude ratios and phase differences could be used for different applications, e.g., breast, liver, and cardiac imaging, without the need to determine patient-specific values. However, as illustrated in Figure 5 studies have shown that this approach was too simplistic, as there was significant variation in
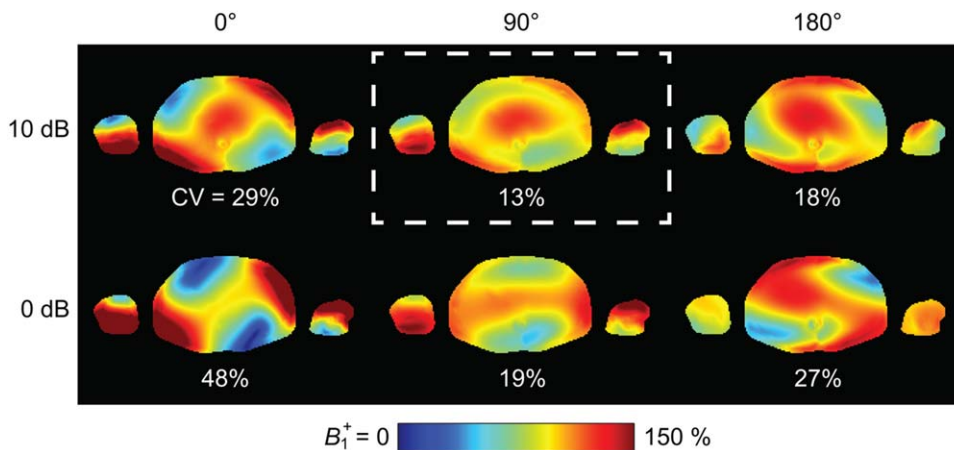
FIGURE 6: Simulations of the effect of B$_1$-shimming on the B$_1$ transmit field. The vertical axis denotes the relative power ratio, and the horizontal axis the relative phase of the two channels. The transverse B$_1$ field is illustrated through the centre of the torso at the level of the liver (superior/inferior direction). The simulation was performed using the Ella model of a normal-sized woman[77] with 75 tissue types, and the maps were normalized to the mean B$_1$. The white box corresponds to the case of the lowest CV, i.e., the highest B$_1$ homogeneity.
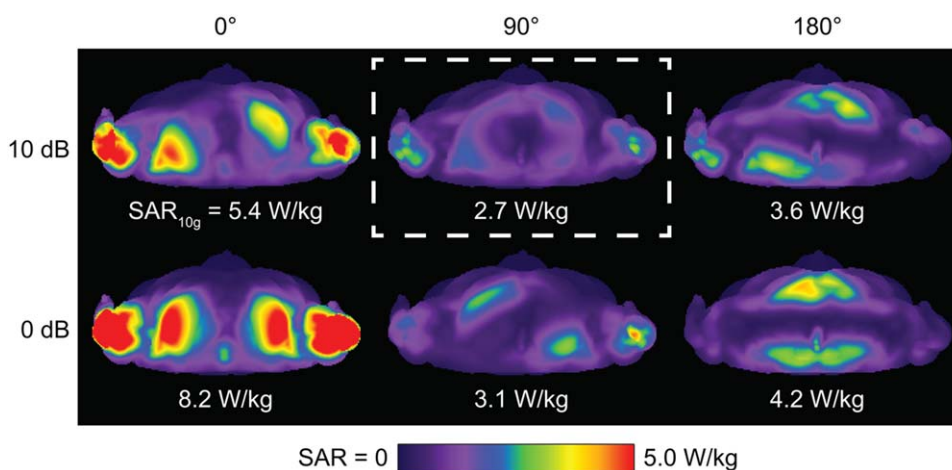
FIGURE 7: Simulation examples of the effect of B_1-shimming on the local SAR. Shown are the transverse maximum intensity projections of the 10 g-averaged SAR for different driving conditions. All data is normalized to a mean B_1 of 1 μT in the transverse plane. The white box corresponds to the case of the lowest SAR.

imaging performance between patients.[11] Therefore, most studies are now performed using patient-specific settings. The process of optimizing image quality by adjusting the amplitudes and phases of the two channels is often referred to as "B_1-shimming." A short additional calibration scan (typically lasting less than a minute) is added to the start of the clinical protocol to map the B_1 field within the patient, and based upon this scan the optimum relative phases and magnitudes feeding the two ports of the dual-channel transmit coil are calculated. There are many different schemes for fast B_1 mapping[12–14] with different vendors using different sequences.

The dependence of the B_1 field on the amplitude and phase settings in a dual channel system is illustrated in Figure 6, which shows that moderate differences can have quite dramatic effects on the spatial distribution of the RF field: simulations were performed as described in Brink and Webb.[15] A 2.5 mm isotropic grid was used with commercially available simulation software (xFDTD 7.2, Remcom Inc., State College, PA). A two-port-drive high-pass birdcage structure was used and the coefficient of variance (CV) of the B_1 homogeneity was calculated for each case. In the case shown in Figure 6 the highest B_1 homogeneity, i.e., the lowest value of the CV, corresponds to a quadrature phase relationship with a 10 dB power difference between the two channels.

In addition to the homogeneity of the B1 transmit field, the other critical component is the specific absorption raio (SAR), covered in the next section. This often sets the limits for the total time that a particular scan can take.

Specific Absorption Ratio

Heat is created in the body by the interaction of the electric field component of the EM field generated by the transmit coil with the conductive elements (tissue, blood, skin) of the body. The power deposited in the body is quantified in terms of the SAR measured in Watts/kg. The SAR is proportional to the product of the conductivity and the square of the electric field. The two different SAR measures relevant to clinical MR scanning are the local 10 g SAR and whole body SAR. As the terms suggest the local SAR is defined as the peak SAR value after spatial averaging over any 10 g of tissue, whereas the whole body SAR is spatially averaged over the entire body. In the United States, the Food and Drug Administration (FDA) limits are: whole-body average 4 W/kg over 15 min, head/trunk local (1 g tissue) 8 W/kg over 10 min, extremities (1 g tissue) 12 W/kg over 5 min.[16] The International Electrotechnical Committee (IEC) has three levels, with all values over a 6-min average: normal (all patients), whole body average 2 W/kg, head/trunk local 10 W/kg and extremities local 20 W/kg; first level (supervised) 4 W/kg, 10 W/kg, and 20 W/kg, respectively; second level (institutional review board approval) 4 W/kg, >10 W/kg and >20 W/kg, respectively.[17]

These safety limits ultimately pose constraints on the values of different imaging parameters such as the flip angle or minimum TR. In practice, the MRI system will not start or will abort the scan if either the IEC-60601-2-33 6-min or 10-s limit (the SAR over any 10-s period is not allowed to exceed twice the levels listed previously) for global or local SAR is exceeded. Using a body coil transmit at 3T, as discussed by many publications, the local SAR limits constrain the imaging parameters before the whole body SAR limit is reached.

In general, SAR is predicted by the MR scanner based on the particular sequence being run. For single-channel transmit systems, these estimates incorporate a set of body models simulated at different landmarks within the system, from which the worst-case scenario (i.e., the maximum possible local SAR as a function of both body model and
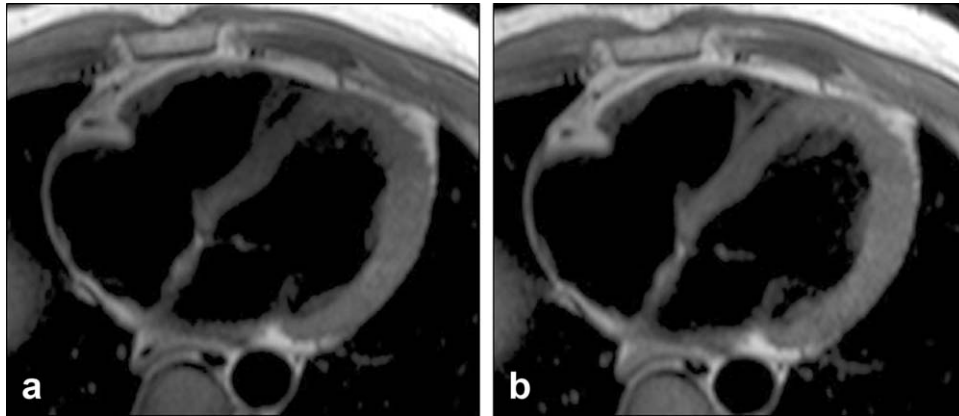
FIGURE 8: Axial TSE BB images (TR 2000 ms, TE 90 ms) obtained with single-channel transmit (a) and dual-channel transmit (b) in a 39-year-old man suspected of having arrhythmogenic right ventricular cardiomyopathy. Note the improved signal homogeneity of the image acquired with RF shimming, which enables clear delineation of the inter-ventricular septum and the anterior free wall of the right ventricle. Figure reproduced with permission from.[31]

landmark) provides a very conservative estimate of the local SAR. The SAR estimate is then coarsely calibrated by measuring the global B_1, i.e., as a single value for the entire imaging volume. In contrast, the more elaborate calibration procedure mandatory for B_1 shimming in a dual-channel transmit system provides a more reliable estimate of the local SAR, because the B_1 field is actually measured, meaning that these additional safety margins can be reduced. Furthermore, the effect of B_1 shimming has been shown to be typically coincident with a reduction of local SAR. This is illustrated in Figure 7, which shows transverse maximum intensity projections of the 10 g-averaged SAR, in which the same driving conditions for the RF coil were applied as in Figure 6. As can be seen from both figures, the driving condition that improves B_1 homogeneity also reduces local SAR. This means that in many cases, the local SAR in the B_1-shimmed case is actually lower than in the single-channel transmit configuration, even if the total amount of power deposited within the body is higher. In this situation the imaging sequence parameters can be "improved" by, for example, decreasing the minimum TR, increasing the number of slices, or increasing the flip angle. The SAR behavior of multi-channel transmit systems is an important advantage and has been investigated by many groups.[18–21]

Clinical Applications

The first extensive clinically oriented reports on the advantages of dual-channel transmit MRI was by Willinek et al[22] who investigated several different application areas. They determined that fast spin-echo images of the liver showed significantly better image homogeneity with dual-channel transmit, as did diffusion-weighted liver imaging. The effect was particularly pronounced in three patients with ascites. The total imaging time could be reduced by one-third due to the reduced maximum local SAR. For scans of the lumbar spine, reductions of 50% in total imaging time for sagit-

tal T_2-weighted and 18% for sagittal T_1-weighted scans were achieved. This pivotal study formed the basis for many subsequent investigations of dual-transmit performance, which are summarized according to organ in the following sections.

Cardiac

Cardiac imaging at 3T has shown significant benefits compared with 1.5T in applications such as myocardial tagging and myocardial perfusion measurements.[23–25] However, in conventional functional protocols using cine sequences and single-channel transmit, the decreased B_1 homogeneity over the heart at 3T reduces image contrast compared with 1.5T. Sung and Nayak[26] have reported that the magnitude of the B_1 field can vary by up to 50% across the heart at 3T. For
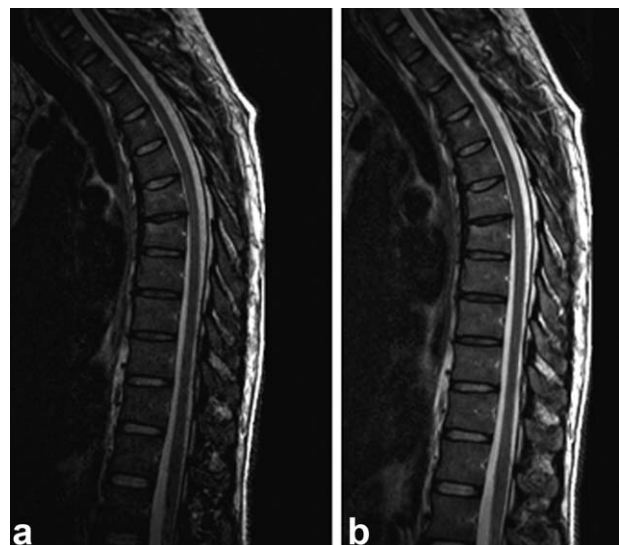

FIGURE 9: Comparisons of single-channel and dual-channel transmit in the spine. a: Sagittal single-channel images acquired in 5 min. b: Corresponding dual-channel images acquired in 3 min with a reduced TR and showing greater image contrast uniformity.
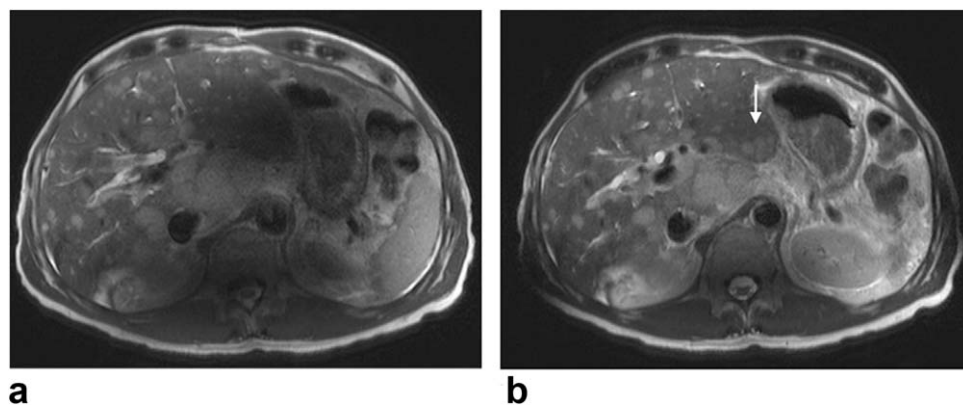
FIGURE 10: Metastatic pancreatic tumor in a 52-year-old man. a: Transverse T$_2$-weighted TSE image acquired using single-channel transmit. There are marked signal loses in the left lobe of the liver and dorsal parts of the right lobe of the liver. Image quality was rated as poor and lesion conspicuity moderate by two readers. b: Corresponding image acquired with dual-channel transmit. Image quality and lesion conspicuity were rated as good by both readers. One additional confluent liver metastasis in Couinaud liver segment II (arrow) was identified by both readers. Figure reproduced with permission from Kukuk et al.[44]

single-channel transmit 3T systems, the minimum TR is greater than that at 1.5T due to the local SAR constraints. In addition to increased scan times, the longer TR increases the sensitivity of the technique to banding artifacts in balanced steady state free precession (bSSFP) sequences, which are the mainstay of cardiac scanning at 1.5T.[27] Despite several authors having shown that there is an increased SNR and contrast-to-noise ratio (CNR) at 3T, the nonuniform flip angle distribution results in sections of the free right ventricular wall and the mid-ventricular and apical septum being obscured.[28,29] The approach of using preset RF shims[30] was initially proposed, but was not found to be particularly effective, because patient size and the presence of sternal wires, pericardial effusions and pleural effusions, amongst other phenomena, strongly affect the B$_1$ spatial distribution within the heart. Therefore, B$_1$-shimming is performed for each individual patient.

The first in-depth investigation of dual-channel transmit cardiac MRI was by Mueller et al.[31] A cardiac-triggered B$_1$ calibration scan was run for each subject using the saturated dual-angle method (SDAM) with segmented echo planar imaging (EPI) readout within a single breath-hold.[12] The mean percentage of the achieved flip angle with dual-channel transmit was $91.9 \pm 3.3\%$ versus $72.8 \pm 4.0\%$ for single-channel transmit. The CNR between the basal interventricular septum and blood pool increased from 26.3 ± 3.4 to 33.3 ± 3.4 with a bSSFP cine sequences, and from 73.0 ± 6.0 to 87.3 ± 5.8 with a turbo spin echo (TSE) black-blood (BB) sequence. In terms of image quality, the contrast between papillary muscles and/or myocardium and the blood pool was significantly increased, and the signal drop-off in the septum, right ventricle, and right ventricular free wall were reduced, as shown in Figure 8. The TR could be significantly reduced, which led to a decrease in banding artifacts from bSSFP sequences.

Jia et al[32] extended the analysis of dual-channel versus single-channel transmit by investigating how the reduced local SAR using dual-channel transmit enabled either an increased value of the flip angle or a decreased TR to be used. In their analysis, the TR could be reduced from 3.4 ms to 2.8 ms for a fixed flip angle of $45°$ in short-axis ventricular cine scans, or alternatively the TR could be maintained at 3.4 ms and the flip angle increased to $58°$. Krishnamurthy et al[11] investigated the performance of a dual-channel transmit system for subjects with different body mass indices (BMIs). The authors showed increased B$_1$ homogeneity, image quality, SNR and CNR for the dual-channel transmit approach, confirming the data from previous studies. In addition, they found that the B$_1$ inhomogeneity from a single-channel system was not correlated to the BMI (or associated measures such as body surface area and width ratio) of the subject. Indeed, they also found that the degree of improvement in B$_1$ homogeneity using the dual-channel transmit approach was also not correlated to these measures. These findings provide further evidence that a patient-specific B$_1$-shimming approach, rather than using predetermined fixed values, is most appropriate.

In a study on high-dose dobutamine stress (HDDS) at 3T, Strach et al[33] also found significant improvements in image and diagnostic quality using a dual-channel transmit system. In the HDDS study (n = 13), all 13 cases were found to be diagnostic in dual-channel transmit mode, compared with only 5 of 13 with single-channel transmit. HDDS studies are potentially affected even more than standard clinical scans by bSSFP image artifacts due to the significant increase in heart rate, and, therefore, more complex and greater blood flow, which in turn result in greater ΔB_0-induced image artifacts for a given TR. The fact that the TR can be reduced in dual-channel transmit mode is, therefore, particularly important in this type of application.
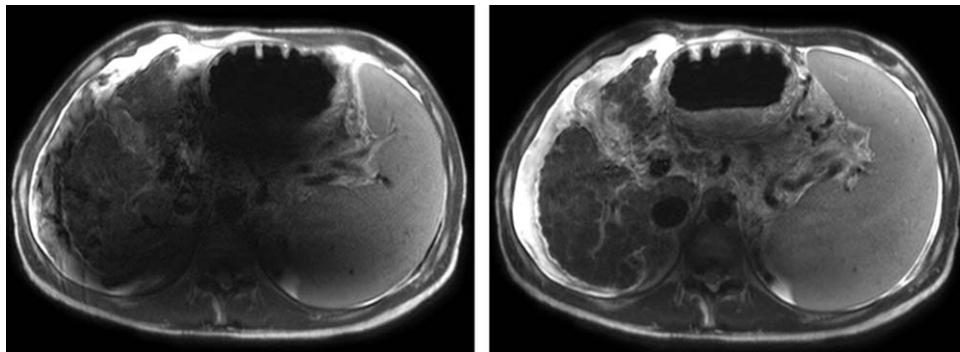
FIGURE 11: Example of image improvement by means of dual-channel transmit from a patient with ascites. A T_2-weighted TSE sequence was run with spatial resolution 1.2 × 1.4 × 7 mm within a single breathhold of 14 s. Left: Single-channel transmit. Right: Dual-channel transmit.
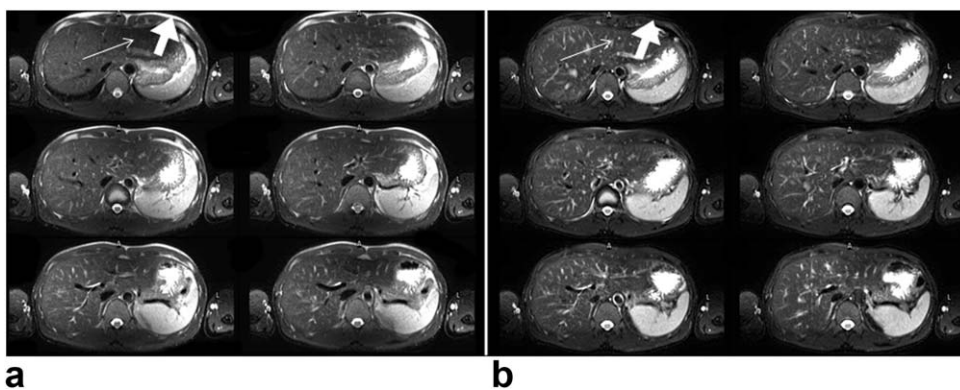
FIGURE 12: a,b: An example of improved image uniformity (thin arrow) and also fat suppression (thick arrow) using dual-channel transmit and a T_2-weighted TSE sequence with SPAIR fat suppression.
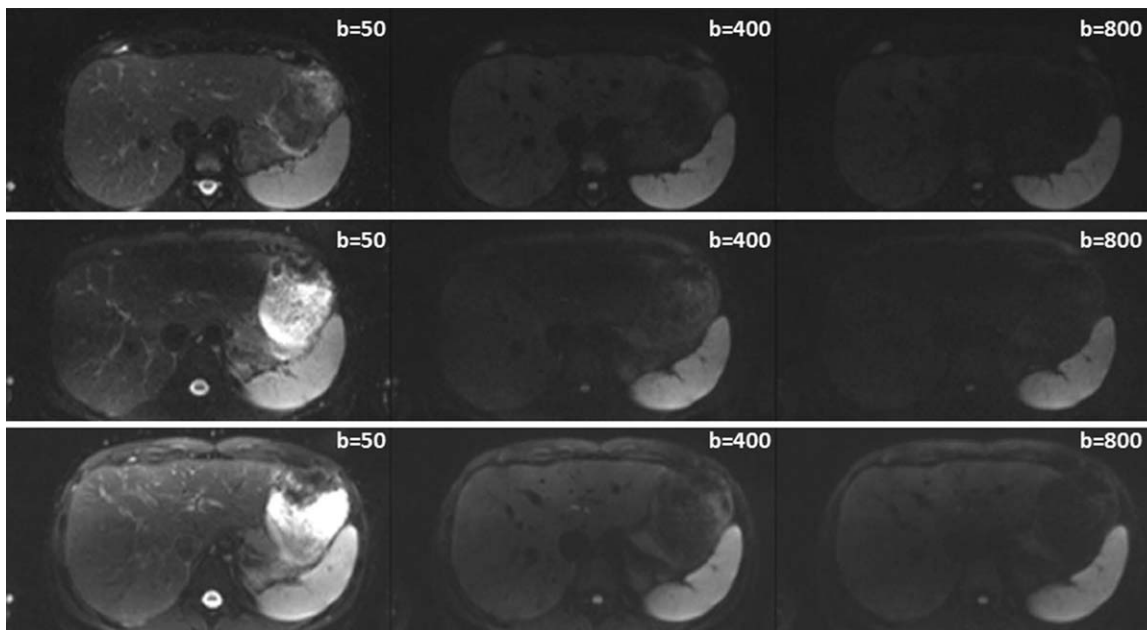
FIGURE 13: Representative images from healthy volunteers acquired at 1.5T (top row), using a single channel transmit 3T (middle row), and using a dual-channel transmit 3T (bottom row). From left to right within each row, b-values increase from 50 to 400 to 800 s/mm^2. Reproduced with permission from Riffel et al.[48]
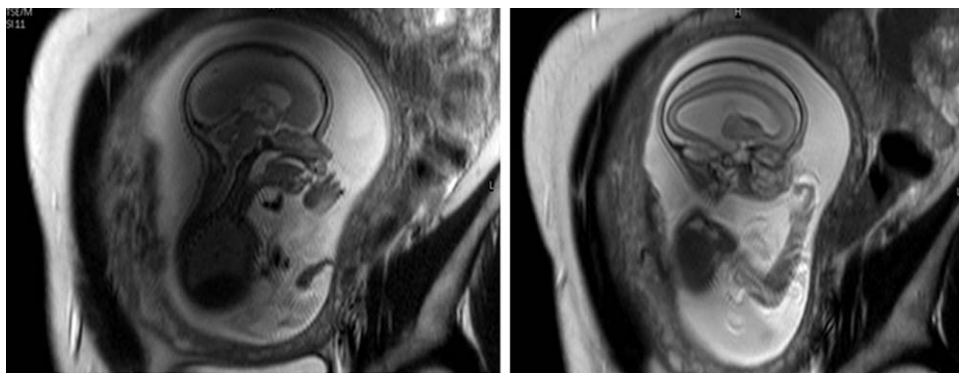
FIGURE 14: Comparison between single-channel (left) and dual-channel (right) single shot spin echo images of a fetus. The single-channel images shows a very low signal intensity in the centre of the image, with much reduced contrast in the fetal brain. This is due to a large amount of amniotic fluid, combined with the large size of the patient. The dual-channel transmit approach improves the diagnostic image quality substantially.

Musculoskeletal

The first application of dual-channel transmit MRI in the spine was presented by Nelles et al.[34] The authors showed that the duration of a three-station examination of the entire vertebral column could be reduced by, on average, a factor of one-third due to the shorter TR values enabled by the reduced local SAR estimate when using dual-channel transmit. Sagittal T_2-weighted scans had a reduction in TR from 3496 to 1748 ms, sagittal T_1-weighted scans from 812 to 578 ms, and sagittal spectral adiabatic inversion recovery (SPAIR) scans from 3554 to 2495 ms. Qualitative analysis showed that the diagnostic imaging quality was comparable to that from the single-channel transmit. In the same study, the authors reported that the transmit power was raised by a mean value of 68% for dual-channel transmit compared with single-channel transmit, while remaining within SAR limits, and produced the same maximum transmit field. However, the root-mean-square (RMS) of the magnitude of the B_1 field was increased by an average of 29% using the dual-channel transmit approach, showing that a higher transmit homogeneity and average efficiency had been achieved.

In routine clinical practice, the reduced total imaging time is particularly important in spine applications due to patient discomfort from lying still for long periods of time: images showing slightly improved image quality even when using reduced imaging times using dual-transmit are shown in Figure 9.

A follow-up study provided further quantitative analysis of single-channel versus dual-channel transmit mode in the lumbar spine.[35] In this case, the authors kept the TR value the same for both cases: however, because the local SAR estimates were reduced using dual-channel transmit, they were able to scan more slices in each TR interval, which halved the imaging time for their axial T_2-weighted and axial T_1-weighted scans. Qualitative assessment by two

neuroradiologists showed that both judged $\sim$90% of the scans (axial T_1-weighted, axial T_2-weighted, sagittal T_1-weighted, and sagittal T_2-weighted) to be superior for the dual-channel transmit mode. Measures of the CNR and SNR showed improvements of 53% and 19% (sagittal T_1), 48% and 23% (axial T_1), 38% and 20% (sagittal T_2), and 100% and 18% (axial T_2), respectively.

The same group has recently used a dual-channel transmit system for producing quantitative $T_1\rho$ maps, which are representative of the distribution of proteoglycan content, in the lumbar spine disk spaces.[36] The authors showed that the dual-channel transmit approach allowed them to use much thinner slices (3 mm) as opposed to 8 mm using the single-channel approach, thus reducing partial-volume effects. Using dual-channel transmit it was possible to run a three-dimensional sequence within SAR limits. In contrast, only a 2D multi-slice sequence was possible in single-channel transmit mode. The reduction in estimated SAR enabled more rapid acquisition of individual images, each one acquired with a specific spin-lock period. This meant that a greater number of images could be acquired within a given total scan duration, which led to a more accurate quantification of the $T_1\rho$ images.

Body Imaging

As noted by many researchers, the intrinsic increase in SNR in body imaging by moving from 1.5T to 3T is often offset by a greater extent of signal loss and inhomogeneous image contrast,[37–43] rendering the higher field images less diagnostically useful. Dual-channel transmit technology has made a substantial contribution to restoring the advantages of the higher field. Kukuk et al,[44] using axial T_2-weighted single-shot turbo spin echo (TSE) sequences, showed significant improvement in the detection of liver lesions using dual-channel compared with single-channel transmit, in addition to improved lesion conspicuity, lesion contrast and general
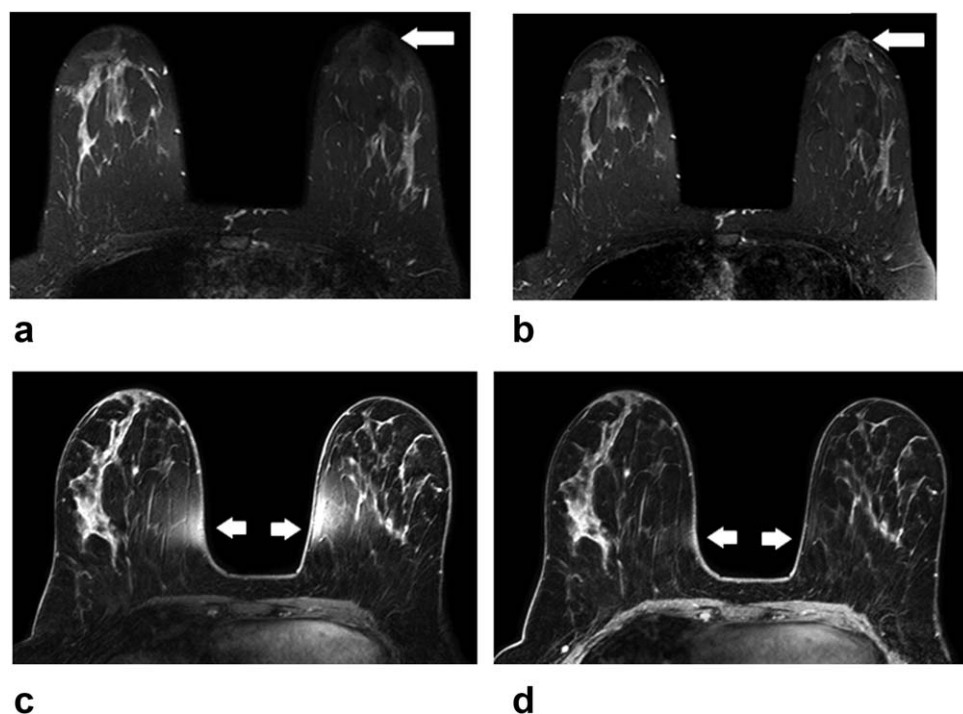
FIGURE 15: a: Single-channel transmit T$_2$-weighted sequence with SPAIR fat suppression, spatial resolution 1 × 1.3 × 2.5 mm. There is a significantly lower signal intensity and image contrast in the right breast compared with the left (arrow). **b:** Corresponding dual-channel transmit shows a much more homogeneous signal intensity and increased image contrast. **c:** 3D T$_1$-weighted high-resolution isotropic volume excitation (THRIVE) sequence, 0.9 × 0.9 × 0.9 mm spatial resolution. The single-channel transmit shows significant image artifacts from incomplete fat suppression (arrows). **d:** Corresponding images using dual-channel transmit show much more homogeneous fat suppression.

image quality. An example is shown in Figure 10, which displays significantly improved image quality in segment 3 of the liver, with an increase in lesion conspicuity and detection (white arrow). Luo et al[45] have also shown significant improvements in liver imaging using a dual-channel transmit approach.

As mentioned earlier, image quality degradation at 3T is particularly severe with patients with ascites, a pathological condition in which large volumes of fluid accumulate in the abdomen. Because ascites is normally a product of pathologies such as liver cirrhosis or neoplasms, it is important to be able to image the affected organs for diagnosis. The fluid has a very high permittivity and conductivity, and, therefore, has a very severe deleterious effect on the B$_1$ homogeneity. An example of how dual-channel transmit can improve image quality is shown in Figure 11.

The increased homogeneity of the transmit field also enables improvements in fat suppression, as illustrated in Figure 12, even for methods such as SPAIR which have an "in-built" robustness with respect to B$_1$ inhomogeneity due to the use of an adiabatic pulse.

Diffusion-weighted abdominal imaging is another area that has shown significant improvement when using the dual-channel transmit approach.[46,47] Any B$_1$ inhomogeneity present not only reduces the image intensity but incomplete fat suppression, as a result of spatially varying flip angles, can cause significant ghosting in the images. Riffel et al[48] showed that images acquired using a dual-channel transmit 3T were of higher quality than those acquired at 1.5T, and both were better than those acquired with a single-channel transmit 3T system, as demonstrated in Figure 13. In a similar study by Rao et al,[49] diffusion coefficients determined using dual-channel transmit at 3T were found to be almost identical to those measured at 1.5T, the current gold standard. This is in stark contrast to the case using single-channel 3T systems, where the values obtained are not currently considered to be reliable.[50]

Diffusion-weighted whole-body imaging with background body signal suppression (DWIBS) is another technique that has been explored using dual-channel transmit at 3T. DWIBS has been used for several different, mainly oncological applications.[50–53] In a trial involving 40 subjects, using dual-channel transmit compared with single-channel transmit, Murtz et al[46] showed that signal homogeneity was improved in 25/40 cases and was equal in 15/40 cases, and fat suppression improved in 17/40 and was equal in 23/40 cases. In addition, the total scan time per patient was reduced by approximately one-third. The image
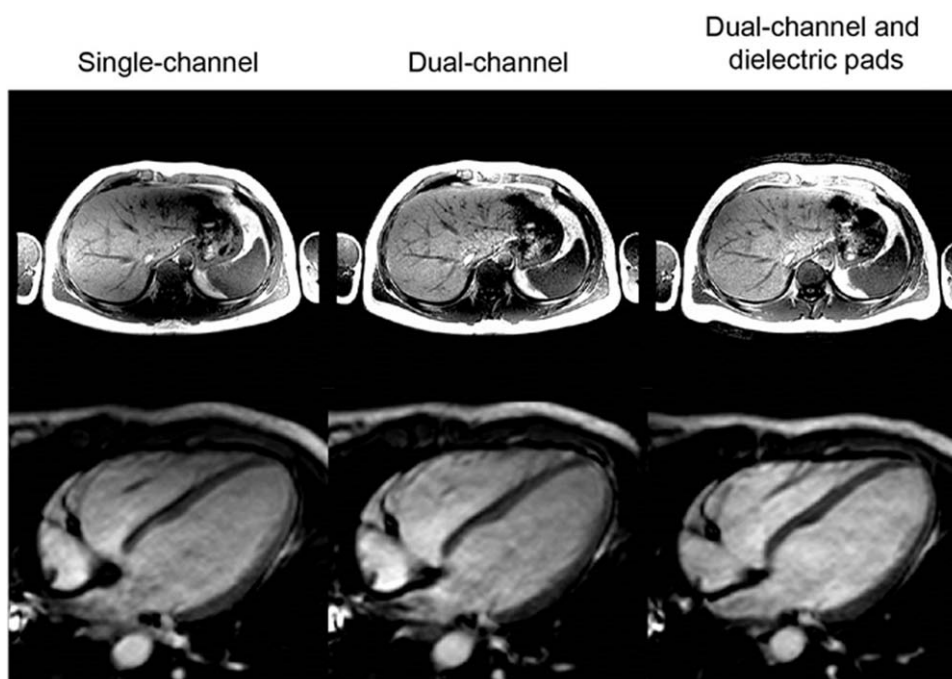
FIGURE 16: Top: Comparison of image quality in an abdominal scan using a single-channel, dual-channel, and dual-channel with high permittivity pads, the last of which gives the highest imaging consistency (ref). Bottom: Similar images from a cardiac scan at 3T, again showing the most consistent image quality from the combined approach.[15]

homogeneity improved in 50% of the pelvis cases, 100% of the abdominal cases, 67% of the chest cases, and 60% of the neck cases: in all other cases the images were judged to be equal. Fat suppression was improved in 33% of the pelvis cases, 50% of the abdominal cases, 83% of the chest cases: in all other cases the images were judged to be equal.

Fetal Imaging

Ultrasound is currently the main imaging modality used to diagnose disorders related to pregnancy. However, fetal MRI is increasingly being used because the quality of ultrasonic imaging is highly dependent on the maternal body habitus and fetal position. Additionally, visualization of the brain using MRI is not restricted by the bony structure of the skull. Soft tissue contrast is better in MR images and abnormally large fetuses can also be studied. However, fetal MR imaging at 3T is particularly sensitive to transmit field inhomogeneities because large volumes of high permittivity and high conductivity liquid, primarily amniotic fluid, are often present. In this case, the added flexibility of dual-channel transmit systems often results in significantly improved image quality. Figure 14 shows a comparison between single-channel and dual-channel transmit for a single shot spin echo sequence at 3T.

Breast Imaging

Left–right differences in image intensity and contrast in imaging the breast are well-known to hamper diagnosis.[54] Fat-suppression also varies spatially, which can cause problems in detecting small lesions. Dual-channel transmit is

very effective in reducing both of these types of image artifact, as shown in Figure 15.

Current State-of-the-art and Future Advances

Dual-channel 3T transmit systems are now offered by most major MR manufacturers, and B1-shimming algorithms are implemented as simple extra calibration scans at the beginning of each examination. Comparison studies with single-channel 3T systems have shown significantly improved diagnostic quality in many applications. Because technology never stands still, we consider here several different areas which may well expand in the future.

Improved and More Rapid B_1 Mapping

A key component to obtaining optimum image quality is the accuracy of the B_1 map produced by the B_1-calibration sequence, which should also be extremely fast to enable implementation in the clinical routine. Current protocols include methods such as dual-TR and dual tip angle[12,14] which are not particularly rapid. However, this is an area of active research, with several new schemes being developed which result in higher sensitivity, more rapid data acquisition and lower SAR: these include using the Bloch-Siegert effect[55] and very rapid dual-stimulated echo approaches.[13] Many of the current sequences are very accurate in mapping areas in which the transmit field is high, but are relatively inaccurate in areas with very low transmit efficiency, which are of course the areas that most need to be improved. B_1-
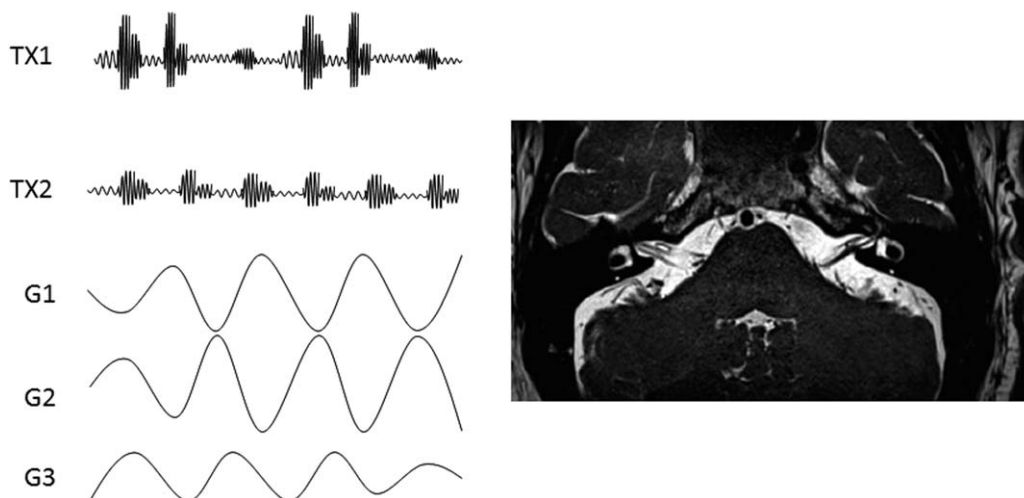
FIGURE 17: Left: Imaging sequence using the full flexibility of a dual-transmit channel system. Completely independent RF waveforms are used for each channel, with appropriate waveforms on all gradient amplifiers for the particular application. Right: Zoomed image of the internal auditory canal from Boada et al.[78]

mapping sequences with greater "dynamic range" are, therefore, needed to improve the B_1 calibration quality, and consequently the B_1 shimming performance.[56]

Accurate SAR Estimation

The estimation of local SAR must be performed extremely rapidly for regular clinical practice. Having determined the B_1-shimmed values of the amplitudes and phases of the two independent transmit channels, these values are then used to predict the SAR based on a precalculated SAR database. For a two-channel system, this consists of a simple lookup-table with various shim settings and corresponding SAR values. To better manage the increasing complexity of these SAR models, which can be especially challenging when considering systems with an even higher channel count (>2), so-called Q-matrices have been introduced.[18] A database consisting of a subset of these Q-matrices can then be built up for a set of different subject models (e.g., adult/child, male/female, high/low BMI, tall/short), to provide a rapid estimate of the SAR. The major disadvantages of this approach is that Q-matrices need to be computed for idealized body models rather than being patient specific, and they do not account for positional differences (e.g., the patient lying asymmetrically). The computational complexity can also be reduced by methods such as the virtual-observation-point approach.[57] The ultimate aim is to be able to produce an accurate estimate of local SAR based upon, for example, the rapid "localizer prescans" used in every clinical protocol.

Combination with Other Approaches

An alternative, and ultimately complementary, approach to overcoming the conductivity and dielectric effects is the use of high permittivity "dielectric pads." Commercial pads consisting of water-based gels are currently available from some vendors. However, with a relative permittivity of $\sim$80, and a thickness up to $\sim$4 cm these are rather bulky while only providing a

moderate correction of the B_1 field.[8,58] Much higher permittivity materials ($\sim$300) made from an aqueous suspension of barium titanate[59,60] have recently been introduced for body imaging at 3T.[9] De Heer et al[9] showed significantly enhanced contrast homogeneity in liver scans using two symmetrically placed (anterior/posterior) 1 cm thick pads. Brink and Webb[15] have shown that cardiac imaging can be improved by reducing SAR by as much as 50% while increasing B_1 homogeneity by using an asymmetric anterior/posterior pad configuration. Both studies indicated that the most consistent imaging quality is obtained by a combination of dual-channel transmit and high permittivity pads, stressing the complementary nature of the two approaches, as demonstrated in Figure 16.

Although there are several advantages of such an approach, most particularly the fact that it is platform-independent and requires no alterations to imaging sequences etc., there are issues of dielectric placement and patient comfort which need to be considered if these are to be used routinely in clinical practice.

Development and Evaluation of Parallel Transmit SENSE

In contrast to the approach of driving the two channels of the body coil with the same RF pulse shape, independent RF waveforms can be transmitted from each channel: this technique is referred to as "parallel transmit" or "transmit SENSE".[61–63] In general, this approach enables one to improve the performance of spatially selective multidimensional RF pulses by reducing their length (therefore, reducing T_2^* decay and off-resonance effects), enhancing their spatial definition (for reduced field-of-view imaging), or reducing the RF power deposited in the patient.

Reduced field-of-view imaging, using multidimensional RF pulses in combination with shaped gradients, is a

method to increase the spatial resolution achieved per unit data acquisition time.[64–66] It is also a useful technique for minimizing motion artifacts from outside the reduced field-of-view. However, the RF pulses required for this type of application are quite long and this results in the images being very sensitive to artifacts caused by magnetic field inhomogeneities. The length of the pulses can be reduced by transmitting different waveforms on the two different channels. For dual-channel transmit systems the pulse lengths can be approximately halved. This has recently been implemented for zoomed imaging by Siemens under the tradename Syngo ZOOMit, as shown in Figure 17.

The second important application of transmit SENSE is to increase the B_1 homogeneity compared with B_1-shimming which forms the basis of all of the clinical studies outlined earlier in this study. Transmit SENSE gives an additional degrees of freedom for increasing the B_1 homogeneity[67] because two separate waveforms can be used. Several different mathematical methods have been presented for optimizing the pulse shapes of each individual RF pulse and the corresponding gradient waveforms.[63,67–69] Finally, transmit SENSE can be used either to reduce the local SAR[70,71] by means of minimizing the mean RF power, or to minimize the peak power required for the RF pulses.[72]

The natural extension of the advantages afforded by dual-channel transmit is to increase the channel count further. Potential advantages are: (i) further reduced local SAR allowing shorter overall scan times, (ii) further increases in the B_1 homogeneity and image contrast, and (iii) increased flexibility for reduced field-of-view imaging using shorter RF pulses, with the imaging volume more closely matching the geometry of the organs of interest. The major disadvantages are the added complexity of the system, the need for sophisticated multi-element transmit arrays, and the increased computational time for SAR calculations. The architecture of an eight-channel system, with eight independent sources, designed for operation at 3T was described many years ago by Vernickel et al.[70] In recent work, Childs et al[73] showed that there was an increase in B_1 homogeneity with increasing channel count, although the greatest increase is achieved by going from single- to dual-channel transmit. There is a large literature dealing with the system architecture for body imaging at 7 Tesla, with between 8 and 32 transmit channels.[74–76] However, such developments at 3T will require significant financial and resource investment from the major commercial MR vendors, and whether the advantages outweigh the costs remains to be seen.

Acknowledgements

References

1. Hayes CE, Edelstein WA, Schenck JF, Mueller OM, Eash M. An efficient, highly homogeneous radiofrequency coil for whole-body NMR imaging at 1.5-T. J Magn Reson 1985;63:622–628.

2. Vaughan JT, Adriany G, Snyder CJ, et al. Efficient high-frequency body coil for high-field MRI. Magn Reson Med 2004;52:851–859.

3. Schick F. Whole-body MRI at high field: technical limits and clinical potential. Eur Radiol 2005;15:946–959.

4. Bernstein MA, Huston J III, Ward HA. Imaging artifacts at 3.0T. J Magn Reson Imaging 2006;24:735–746.

5. Chang KJ, Kamel IR. Abdominal imaging at 3T: challenges and solutions. Appl Radiol 2010:22–31.

6. Cornfeld D, Weinreb J. Simple changes to 1.5-T MRI abdomen and pelvis protocols to optimize results at 3 T. Ajr Am J Roentgenol 2008; 190:W140–W150.

7. Sled JG, Pike GB. Standing-wave and RF penetration artifacts caused by elliptic geometry: an electrodynamic analysis of MRI. IEEE Trans Med Imaging 1998;17:653–662.

8. Franklin KM, Dale BM, Merkle EM. Improvement in B1-inhomogeneity artifacts in the abdomen at 3T MR imaging using a radiofrequency cushion. J Magn Reson Imaging 2008;27:1443–1447.

9. de Heer P, Brink WM, Kooij BJ, Webb AG. Increasing signal homogeneity and image quality in abdominal imaging at 3 T with very high permittivity materials. Magn Reson Med 2012;68:1317–1324.

10. Wust P, Nadobny J, Felix R, Deuflhard P, Louis A, John W. Strategies for optimized application of annular-phased-array systems in clinical hyperthermia. Int J Hypertherm 1991;7:157–173.

11. Krishnamurthy R, Pednekar A, Kouwenhoven M, Cheong B, Muthupillai R. Evaluation of a subject specific dual-transmit approach for improving B-1 field homogeneity in cardiovascular magnetic resonance at 3T. J Cardiovasc Magn Reson 2013;15:68.

12. Cunningham CH, Pauly JM, Nayak KS. Saturated double-angle method for rapid B-1 plus mapping. Magn Reson Med 2006;55:1326–1333.

13. Nehrke K, Bornert P. DREAM - a novel approach for robust, ultrafast, multislice B-1 mapping. Magn Reson Med 2012;68:1517–1526.

14. Yarnykh VL. Optimal radiofrequency and gradient spoiling for improved accuracy of T_1 and B_1 measurements using fast steady-state techniques. Magn Reson Med 2010;63:1610–1626.

15. Brink WM, Webb AG. High permittivity pads reduce specific absorption rate, improve B homogeneity, and increase contrast-to-noise ratio for functional cardiac MRI at 3 T. Magn Reson Med 2014;71: 1632–1640.

16. Food and Drug Administration. Guidance for industry and FDA staff: criteria for significant risk investigations of magnetic resonance diagnostic devices. Silver Spring, MD: FDA; 2008.

17. International Electrotechnical Commission. International standard, medical equipment—IEC 60601-2-33: particular requirements for the safety of magnetic resonance equipment for medical diagnosis, 3rd ed. Geneva, Switzerland: International Electrotechnical Commission;. 2010.

18. Graesslin I, Homann H, Biederer S, et al. A specific absorption rate prediction concept for parallel transmission MR. Magn Reson Med 2012;68:1664–1674.

19. Seifert F, Wuebbeler G, Junge S, Ittermann B, Rinneberg H. Patient safety concept for multichannel transmit coils. J Magn Reson Imaging 2007;26:1315–1321.

20. Mao WH, Wang ZW, Smith MB, Collins CM. Calculation of SAR for transmit coil arrays. Concepts Magn Reson Part B Magn Reson Eng 2007;31B:127–131.

21. Van den Berg CAT, van den Bergen B, de Kamer JBV, et al. Simultaneous B-1(+) homogenization and specific absorption rate hotspot suppression using a magnetic resonance phased array transmit coil. Magn Reson Med 2007;57:577–586.

22. Willinek WA, Gieseke J, Kukuk GM, et al. Dual-source parallel radiofrequency excitation body MR imaging compared with standard MR imaging at 3.0 T: initial clinical experience. Radiology 2010;256:966–975.

23. Cheng ASH, Pegg TJ, Karamitsos TD, et al. Cardiovascular magnetic resonance perfusion imaging at 3-Tesla for the detection of coronary artery disease - a comparison with 1.5-Tesla. J Am Coll Cardiol 2007;49:2440–2449.

24. Cheng ASH, Pegg TJ, Karamitsos TD, et al. The utility of cardiovascular magnetic resonance perfusion imaging at 3 Tesla for detection of coronary artery disease: a comparison with 1.5 Tesla. Eur Heart J 2007;28:275–275.

25. Thomas D, Strach K, Meyer C, et al. Combined myocardial stress perfusion imaging and myocardial stress tagging for detection of coronary artery disease at 3 Tesla. J Cardiovasc Magn Reson 2008;10:59.

26. Sung K, Nayak KS. Measurement and characterization of RF nonuniformity over the heart at 3T using body coil transmission. J Magn Reson Imaging 2008;27:643–648.

27. Barkhausen J, Ruehm SG, Goyen M, Buck T, Laub G, Debatin JF. MR evaluation of ventricular function: true fast imaging with steady-state precession versus fast low-angle shot cine MR imaging: feasibility study. Radiology 2001;219:264–269.

28. Greenman RL, Shirosky JE, Mulkern RV, Rofsky NM. Double inversion black-blood fast spin-echo imaging of the human heart: a comparison between 1.5T and 3.0T. J Magn Reson Imaging 2003;17:648–655.

29. Gutberlet M, Noeske R, Schwinge K, Freyhardt P, Felix R, Niendorf T. Comprehensive cardiac magnetic resonance imaging at 3.0 tesla - feasibility and implications for clinical applications. Invest Radiol 2006;41:154–167.

30. Zhai Z, De Meester GD, Morich MA, Harvey PR; MR involving high speed coil mode switching between I-channel linear, Q-channel linear, quadrature and anti-quadrature modes. Patent WO2007/12426. 2007.

31. Mueller A, Kouwenhoven M, Naehle CP, et al. Dual-source radiofrequency transmission with patient-adaptive local radiofrequency shimming for 3.0-T cardiac MR imaging: initial experience. Radiology 2012;263:77–85.

32. Jia HP, Wang CY, Wang GB, et al. Impact of 3.0 T cardiac MR imaging using dual-source parallel radiofrequency transmission with patient-adaptive B1 shimming. Plos One 2013;8:e66946.

33. Strach K, Clauberg R, Muller A, et al. Feasibility of high-dose dobutamine stress SSFP cine MRI at 3 Tesla with patient adaptive local RF shimming using dual-source RF transmission: initial results. Rofo 2013;185:34–39.

34. Nelles M, Konig RS, Gieseke J, et al. Dual-source parallel RF transmission for clinical MR imaging of the spine at 3.0 T: intraindividual comparison with conventional single-source transmission. Radiology 2010;257:743–753.

35. Filippi CG, Carlson M, Johnson JM, Burbank HN, Alsofrom GF, Andrews T. Improvements in lumbar spine MRI at 3 T using parallel transmission. AJR Am J Roentgenol 2012;199:861–867.

36. Filippi CG, Duncan CT, Watts R, et al. In vivo quantification of T1 rho in lumbar spine disk spaces at 3 T using parallel transmission MRI. AJR Am J Roentgenol 2013;201:W110–W116.

37. Merkle EM, Dale BM. Abdominal MRI at 3.0 T: the basics revisited. AJR Am J Roentgenol 2006;186:1524–1532.

38. Schindera ST, Merkle EM, Dale BM, Delong DM, Nelson RC. Abdominal magnetic resonance imaging at 3.0 T: what is the ultimate gain in signal-to-noise ratio? Acad Radiol 2006;13:1236–1243.

39. von Falkenhausen MM, Lutterbey G, Morakkabati-Spitz N, et al. High-field-strength MR imaging of the liver at 3.0 T: intraindividual comparative study with MR imaging at 1.5 T. Radiology 2006;241:156–166.

40. Lee VS, Hecht EM, Taouli B, Chen Q, Prince K, Oesingmann N. Body and cardiovascular MR Imaging at 3.0 T. Radiology 2007;244:692–705.

41. Chang JM, Lee JM, Lee MW, et al. Superparamagnetic iron oxide-enhanced liver magnetic resonance imaging - comparison of 1.5 T and 3.0 T imaging for detection of focal malignant liver lesions. Invest Radiol 2006;41:168–174.

42. Ramalho M, Heredia V, Tsurusaki M, Altun E, Semelka RC. Quantitative and qualitative comparison of 1.5 and 3.0 Tesla MRI in patients with chronic liver diseases. J Magn Reson Imaging 2009;29:869–879.

43. Tsurusaki M, Semelka RC, Zapparoli M, et al. Quantitative and qualitative comparison of 3.0 T and 1.5 T MR imaging of the liver in patients with diffuse parenchymal liver disease. Eur J Radiol 2009;72:314–320.

44. Kukuk GM, Gieseke J, Weber S, et al. Focal liver lesions at 3.0 T: lesion detectability and image quality with T2-weighted imaging by using conventional and dual-source parallel radiofrequency transmission. Radiology 2011;259:421–428.

45. Luo ZR, Wang D, Sun XL, Wang GK, Zhuang XJ, Shen BZ. Comparison of dual-source parallel radio frequency transmission liver MRI at 3.0 T with conventional MRI. Minerva Med 2013;104:583–592.

46. Murtz P, Kaschner M, Traber F, et al. Evaluation of dual-source parallel RF excitation for diffusion-weighted whole-body MR imaging with background body signal suppression at 3.0 T. Eur J Radiol 2012;81:3614–3623.

47. Murtz P, Kaschner M, Traber F, et al. Diffusion-weighted whole-body MRI with background body signal suppression: technical improvements at 3.0 T. J Magn Reson Imaging 2012;35:456–461.

48. Riffel P, Rao RK, Haneder S, Meyer M, Schoenberg SO, Michaely HJ. Impact of field strength and RF excitation on abdominal diffusion-weighted magnetic resonance imaging. World J Radiol 2013;5:334–344.

49. Rao RK, Riffel P, Meyer M, et al. Implementation of dual-source RF excitation in 3 T MR-scanners allows for nearly identical ADC values compared to 1.5 T MR scanners in the abdomen. Plos One 2012;7:e32613.

50. Padhani AR, Liu G, Koh DM, et al. Diffusion-weighted magnetic resonance imaging as a cancer biomarker: consensus and recommendations. Neoplasia 2009;11:102–125.

51. Kwee TC, Takahara T, Ochiai R, et al. Whole-body diffusion-weighted magnetic resonance imaging. Eur J Radiol 2009;70:409–417.

52. Kwee TC, Takahara T, Ochiai R, et al. Complementary roles of whole-body diffusion-weighted MRI and 18F-FDG PET: the state of the art and potential applications. J Nucl Med 2010;51:1549–1558.

53. Takahara T, Imai Y, Yamashita T, Yasuda S, Nasu S, Van CM. Diffusion weighted whole body imaging with background body signal suppression (DWIBS): technical improvement using free breathing, STIR and high resolution 3D display. Radiat Med 2004;22:275–282.

54. Kuhl CK, Kooijman H, Gieseke J, Schild HH. Effect of B-1 inhomogeneity on breast imaging at 3.0 T. Radiology 2007;244:929–930.

55. Sacolick LI, Wiesinger F, Hancu I, Vogell MW. B-1 Mapping by Bloch-Siegert shift. Magn Reson Med 2010;63:1315–1322.

56. Brunner DO, Pruessmann KP. B1(+) interferometry for the calibration of RF transmitter arrays. Magn Reson Med 2009;61:1480–1488.

57. Eichfelder G, Gebhardt M. Local specific absorption rate control for parallel transmission by virtual observation points. Magn Reson Med 2011;66:1468–1476.

58. Sreenivas A, Lowry M, Gibbs P, Pickles M, Turnbull LW. A simple solution for reducing artefacts due to conductive and dielectric effects in clinical magnetic resonance imaging at 3 T. Eur J Radiol 2007;62:143–146.

59. Teeuwisse WM, Brink WM, Haines KN, Webb AG. Simulations of high permittivity materials for 7 T neuroimaging and evaluation of a new barium titanate-based dielectric. Magn Reson Med 2012;67:912–918.

60. Teeuwisse WM, Brink WM, Webb AG. Quantitative assessment of the effects of high-permittivity pads in 7 Tesla MRI of the brain. Magn Reson Med 2012;67:1285–1293.

61. Katscher U, Bornert P, Leussler C, van den Brink JS. Transmit SENSE. Magn Reson Med 2003;49:144–150.

62. Zhu YD. Parallel excitation with an array of transmit coils. Magn Reson Med 2004;51:775–784.

63. Katscher U, Bornert P. Parallel RF transmission in MRI. NMR Biomed 2006;19:393–400.

64. Pauly J, Nishimura D, Macovski A. A k-space analysis of small-tip-angle excitation. J Magn Reson 1989;81:43–56.

65. Bornert P, Schaffter T. Curved slice imaging. Magn Reson Med 1996; 36:932–939.

66. Hardy CJ, Cline HE. Spatial localization in 2 dimensions using NMR designer pulses. J Magn Reson 1989;82:647–654.

67. Grissom W, Yip CY, Zhang ZH, Stenger VA, Fessler JA, Noll DC. Spatial domain method for the design of RF pulses in multicoil parallel excitation. Magn Reson Med 2006;56:620–629.

68. Grissom WA, Xu D, Kerr AB, Fessler JA, Noll DC. Fast large-tip-angle multidimensional and parallel RF pulse design in MRI. IEEE Trans Med Imaging 2009;28:1548–1559.

69. Grissom WA, Yip CY, Wright SM, Fessler JA, Noll DC. Additive angle method for fast large-tip-angle RF pulse design in parallel excitation. Magn Reson Med 2008;59:779–787.

70. Vernickel P, Roschmann P, Findeklee C, et al. Eight-channel transmit/receive body MRI coil at 3T. Magn Reson Med 2007;58:381–389.

71. Graesslin I, Niemann M, Harvey P, Vernickel P, Katscher U. SAR and RF power reduction with parallel excitation using non-cartesian trajectories. Magn Reson Mater Phys Biol Med 2005;18:S251.

72. Yip CY, Fessler JA, Douglas CN. Iterative RF pulse design for multidimensional, small-tip-angle selective excitation. Magn Reson Med 2005;54:908–917.

73. Childs AS, Malik SJ, O'Regan DP, Hajnal JV. Impact of number of channels on RF shimming at 3T. Magn Reson Mater Phys Biol Med 2013;26:401–410.

74. Vaughan JT, Snyder CJ, DelaBarre LJ, Bolan PJ, Tian J, Bolinger L, Adriany G, Andersen P, Strupp J, Ugurbil K. Whole-body imaging at 7T: preliminary results. Magn Reson Med 2009;61:244–248.

75. Kraff O, Bitz AK, Kruszona S, et al. An eight-channel phased array RF coil for spine MR imaging at 7 T. Invest Radiol 2009;44:734–740.

76. Graessl A, Renz W, Hezel F, et al. Modular 32-channel transceiver coil array for cardiac MRI at 7.0T. Magn Reson Med 2014; 72:276–290.

77. Christ A, Kainz W, Hahn EG, et al. The Virtual Family-development of surface-based anatomical models of two adults and two children for dosimetric simulations. Phys Med Biol 2010;55:N23–N38.

78. Boada FE, Shepherd T, Rosenkrantz A, et al. Parallel transmission and its clinical implementation: enabling new clinical imaging paradigms. Magnetom Flash 2013;2:104–110.